Aluminum-Doped Zirconia Nanopowders: Chemical Vapor Synthesis and Structural Analysis by Rietveld Refinement of X-ray Diffraction Data

Vladimir V. Srdić*,†,‡,§ and Markus Winterer*,†

Thin Films Division, Institute of Materials Science, Darmstadt University of Technology, Darmstadt, Germany, and Faculty of Technology, Department of Inorganic Technology and Materials Science, University of Novi Sad, Yugoslavia

Received September 23, 2002. Revised Manuscript Received April 7, 2003

Zirconia nanoparticles doped with up to 50 mol % Al_2O_3 were prepared by chemical vapor synthesis (CVS). XRD data of these powders were refined by Rietveld analysis. Doping with alumina decreases the fraction of the monoclinic ZrO_2 phase and stabilizes the tetragonal or cubic ZrO_2 phase, forming different ZrO_2/Al_2O_3 solid solutions. The tetragonal zirconia solid solution is obtained in the as-synthesized nanopowders doped with 3 and 5 mol % Al_2O_3, whereas the cubic zirconia solid solution is formed in the nanopowder with 15 mol % Al_2O_3. Zirconia nanoparticles with higher alumina content (30 and 50 mol % Al_2O_3) are amorphous and crystallize during annealing, forming the single-phase tetragonal ZrO_2 at 800 °C and a mixture of tetragonal ZrO_2 and γ- or η-Al_2O_3 at 850 °C, respectively. During annealing, the stability of the high-temperature zirconia phases decreases considerably with increasing temperature. Thus, the cubic ZrO_2 phase transforms to the tetragonal. The tetragonality (*c*/*a* ratio) and the fraction of the monoclinic ZrO_2 increase with temperature. Zirconia-alumina phase separation is observed in highly doped powders ($\geq$15 mol % Al_2O_3). The observed maximum solubility of alumina in the cubic/tetragonal zirconia is about 15 mol % Al_2O_3 (or 26 at. % Al).

Introduction

The high-temperature modifications of zirconia (tetragonal and cubic) can be stabilized at room temperature with different dopants (MgO, CaO, Y_2O_3, Sc_2O_3, etc.). It is well-known that the stabilization is achieved by incorporation of divalent or trivalent cations in the fluorite-type structure by substitution of Zr^{4+} cations and creation of oxygen vacancies to maintain the local charge balance.[1,2] On the other hand, Al_2O_3 is usually added to zirconia to suppress grain growth during sintering.[3] Due to the much smaller ionic radius of Al^{3+} (0.5 Å) compared to that of Zr^{4+} (0.8 Å), no mutual solubility is generally observed in zirconia/alumina composites produced by conventional methods. However, recent developments of nanoprocessing techniques in which precursors are mixed on the molecular level have enabled the formation of different structures where aluminum ions are incorporated into the zirconium−oxygen network.[4−11] Various methods have been used for the preparation of such zirconia/alumina solid solutions. *Wet-chemical* synthesis is based on the simultaneous hydrolysis of aluminum and zirconium alkoxides[4] or zirconium chloride.[5] In *spray pyrolysis* aqueous solutions of zirconium acetate and aluminum nitrate[8] are used as precursors. Laser evaporation of alumina and zirconia[10] is a *gas-phase synthesis* method where nanoparticles are formed by condensation in the laser-plume above the target. In these samples stabilization of the high-temperature zirconia phases was observed and interpreted as a single-phase solid solution of composition $Zr_{(1-x)}Al_xO_{(2-x/2)}$.[8,10] It is suggested[8] that Al^{3+} ions substitute Zr^{4+} ions, creating oxygen vacancies to maintain local charge balance analogous to other divalent and trivalent cations forming solid solutions with ZrO_2.

In our previous work[12] nonagglomerated, pure, nanocrystalline zirconia powder, with particle sizes of about 5 nm and a size distribution close to monodisperse, was synthesized by chemical vapor synthesis (CVS), a modified chemical vapor deposition (CVD) method. The CVS

* To whom correspondence should be addressed. E-mail: mwinterer@web.de.
† Darmstadt University of Technology.
‡ University of Novi Sad.
§ E-mail: srdicvv@uns.ns.ac.yu.

(1) Li, P.; Chen, I.-W.; Penner-Hahn, J. E. *Phys. Rev.* **1993**, *B48*, 10074.
(2) Li, P.; Chen, I.-W.; Penner-Hahn, J. E. *J. Am. Ceram. Soc.* **1994**, *77*, 118.
(3) Lange, F. F.; Hirlinger, M. M. *J. Am. Ceram. Soc.* **1987**, *70*, 827.
(4) Yamaguchi, O.; Shirai, M.; Yoshinaka, M. *J. Am. Ceram. Soc.* **1988**, *71*, C-510.
(5) Low, I. M.; McPherson, R. *J. Mater. Sci.* **1989**, *24*, 892.
(6) Jayaram, V.; Whitney, T.; Levi, C. G.; Mehrabian, R. *Mater. Sci. Eng.* **1990**, *A124*, 65.
(7) Srdić, V. V.; Radonjic, L. *J. Eur. Ceram. Soc.* **1994**, *14*, 237.
(8) Balmer, M. L.; Lange, F. F.; Levi, C. G. *J. Am. Ceram. Soc.* **1994**, *77*, 2069.
(9) Shi, J. L.; Li, B. S.; Ruan, M. L.; Yen, T. S. *J. Eur. Ceram. Soc.* **1995**, *15*, 959
(10) Ferkel, H.; Naser, J.; Riehemann, W. *Nanostruct. Mater.* **1997**, *8*, 457.
(11) Srdić, V. V.; Winterer, M.; Miehe, G.; Hahn, H. *Nanostruct. Mater.* **1999**, *12*, 95.
(12) Srdić, V. V.; Winterer, M.; Hahn, H. *J. Am. Ceram. Soc.* **2000**, *83*, 729.

10.1021/cm021303q CCC: $25.00
Published on Web 05/31/2003

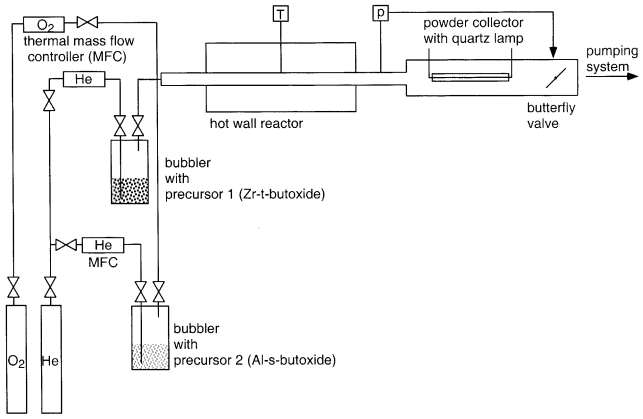

Figure 1. Schematic drawing of the CVS reactor used for the synthesis of the doped zirconia nanopowders.

nanocrystalline zirconia powder was pressureless sintered in vacuum at 950 °C to full dense, transparent, monoclinic zirconia ceramics with an average grain size of 60 nm.[12] It was demonstrated[13] that the grain growth can be additionally suppressed by doping with alumina. Thus, CVS zirconia doped with 3 and 5 mol % Al_2O_3 could be vacuum-sintered at 1000 °C to fully dense, transparent ceramics with an average grain size of 40−45 nm.[13] The aim of the present work is to investigate the effects of alumina dopants on the characteristics of the CVS zirconia nanopowders and to provide further insight into the structure in ZrO_2 doped with Al_2O_3, especially to find evidence for the existence of ZrO_2/Al_2O_3 solid solutions.

Experimental Section

Powder Synthesis. The modular CVS reactor, used for synthesis of nanocrystalline doped zirconia powders, is shown schematically in Figure 1. It consists of two bubblers as the precursor delivery system, a hot wall reactor consisting of an alumina tube with a length of 400 mm (hot zone about 300 mm) and an inner diameter of 19 mm heated by a resistance furnace, a powder collection zone, and a pumping unit. The liquid precursors, zirconium-*tert*-butoxide, ZTB (99.99%, Inorgtech, England), and aluminum-*sec*-butoxide, ASB (>97%, Merck, Germany), held at 80 and 175 °C, respectively, are bubbled with helium (99.996%) as carrier gas. Precursor vapors, carried by helium gas and an additional flow of oxygen (99.995%), are intimately mixed before the reaction is initiated. The mass flows of helium through both bubblers and oxygen are measured and controlled by thermal MKS Instruments mass flow controllers. Different alumina contents (doping level of 0, 3, 5, 15, 30, and 50 mol % Al_2O_3) are achieved by adjusting the mass flows of helium through the bubblers. Additionally, constant oxygen flow of 1000 cm^3/min was used. The continuous gas flow in the system is produced by a combination of a roots pump (250 m^3/h) and a sliding vane pump (65 m^3/h). The total pressure was measured using a Baratron gauge and held constant at 1000 Pa with a butterfly valve. During the short residence time of about 2 ms in the hot zone held at 1000 °C precursor molecules decompose and react, forming small zirconia-doped nanoparticles. In the collection zone, a heated quartz lamp creates a temperature gradient in a cylindrical water-cooled metal tube, where the doped zirconia nanoparticles are separated from the gas stream by thermophoresis. The as-synthesized nanopowders were stored in the glovebox under an inert atmosphere. In a typical experiment, about 3 g of doped nanopowder is obtained per hour, with yields in the range of 55−60%. The yield is defined as the ratio of the mass of as-synthesized powder to the calculated equivalent mass of ZrO_2 and Al_2O_3 in precursors spent during processing. It is mostly limited by the collection efficiency of the thermophoretic collector. The high-temperature behavior of the as-synthesized doped zirconia nanopowders is investigated by annealing in air at different temperatures up to 1100 °C for 3 h.

Table 1. Characteristics of the As-Synthesized CVS Doped Zirconia Nanopowders: Crystallite Size Estimated by XRD (d_{XRD}), Microstrain, and Existing Crystalline Phases

nominal Al_2O_3 content (mol %)	measured Al_2O_3 content (mol %)	d_{XRD} (nm)	microstrain	crystalline phase[a]
0	0	4.8 (5)	0.0041 (7)	t + m (22)
3	2.7	4.5 (4)	0.0093 (15)	t + m (19)
5	5.1	4.9 (3)	0.0163 (22)	t + m (16)
15	16.2	4.1 (6)	0.0128 (15)	c
30	29.5			amorphous
50	52.1			amorphous

[a] t, tetragonal ZrO_2; c, cubic ZrO_2; m, monoclinic ZrO_2. Volume fraction of m-ZrO_2 is given in parentheses.

Powder Characterization. The Al_2O_3 content in the doped zirconia nanopowders was determined by EDX using appropriate standards. The Al_2O_3 contents are close to the nominal values of 3, 5, 15, 30, and 50 mol %, which were used in this paper to label the samples (Table 1). The X-ray diffraction measurements were performed with a Siemens D5000 instrument using Ni-filtered Cu Kα radiation, produced at 40 kV and 30 mA. The XRD data were recorded with a collection mode of 30 s/step and a step size of 0.05° 2θ over the range from 20 to 110° 2θ. Complete analysis of the X-ray data and identification of zirconia and alumina phases was performed using "FullProf", a Rietveld profile-fitting program for multiphase powder XRD data.[14] The background was fit by a six-parameter polynomial and refined simultaneously with the zero-point and scale factor. The modified Thompson−Cox−Hastings pseudo-Voigt profile function was used for the peak shape. No correction was made for preferred orientation and peak asymmetry. Parameters characterizing the instrumental resolution function were obtained from a LaB_6 standard powder sample by the appropriate Rietveld analysis and kept constant during refinements. Refinements were undertaken in space group $P2_1/c$ for monoclinic ZrO_2 with all atoms in general positions, in space group $P4_2/nmc$ for tetragonal ZrO_2 with Zr and O atoms in the special positions 2a and 4d, respectively, and in space group $Fm3m$ for cubic ZrO_2 with Zr and O atoms in the special positions 4a and 8c, respectively. Furthermore, it was assumed that all Al atoms are on Zr sites in the tetragonal or cubic zirconia lattice or that some Al atoms remain in the zirconia lattice and the rest form a separate alumina phase (amorphous and/or crystalline transitional η-, γ-, or θ-Al_2O_3). Occupation numbers were calculated according to the assumption that in both tetragonal and cubic ZrO_2, Al atoms randomly occupy the Zr sites in lattice and charge balance is achieved by formation of vacancies on the O sites. Space group $Fd3m$ is used for the transitional η- and γ-Al_2O_3 phases and $C2/m$ for θ-Al_2O_3. The aluminum contents in the as-synthesized CVS powders are determined by energy-dispersive X-ray analysis (EDX), using a high-resolution scanning electron microscope, HRSEM Philips XL 30 FEG, and appropriate standards.

Results

Characteristics of As-Synthesized Powders. Selected 2θ ranges of X-ray diffraction patterns of the as-synthesized CVS doped powders are shown in Figure 2. The nanopowders doped with 30 and 50 mol % Al_2O_3

(13) Srdić, V. V.; Winterer, M.; Hahn, H. *J. Am. Ceram. Soc.* **2000**, *83*, 1853.

(14) Rodriguez-Carvajal, J. Private communication, Laboratoire Leon Brillouin, Saclay, Gif-sur-Yvette, 1997.

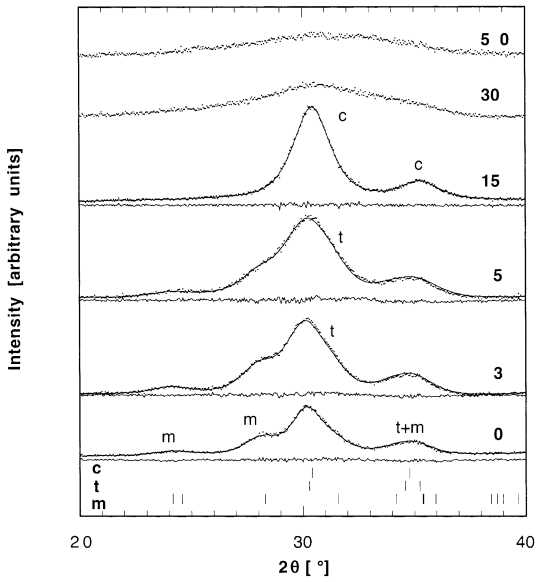

Figure 2. XRD patterns of the as-synthesized CVS doped zirconia nanopowders (letters "t", "c", and "m" denote tetragonal, cubic, and monoclinic zirconia phases, respectively; numbers indicate the alumina content in mol % Al_2O_3). Lines through data points are the best Rietveld refinements and lines below the data are the corresponding residual signals, vertical lines are Bragg positions for the different phases.

are amorphous, whereas the zirconia powders with lower alumina contents ($\leq$5 mol % Al_2O_3) are crystalline, consisting only of zirconia phases without any traces of crystalline alumina (Table 1). Due to the considerable line broadening and overlapping of the corresponding X-ray reflections, the structure of the zirconia phases can only be determined by Rietveld analysis. Refinements were performed with the pure monoclinic ZrO_2 phase, the tetragonal or cubic ZrO_2 structure with different fractions of Al atoms on Zr sites, and the corresponding quantity of the amorphous and/or transitional η- or γ-alumina phase (formed by the rest of the Al^{3+} ions). Refinements with the minimum Bragg R-factor and RF-factor and the maximum DW-stat factor were selected as best fits. For the as-synthesized CVS doped powders best fits were always obtained when all Al atoms are on Zr sites of the dominant zirconia phase, which can be tetragonal (for pure zirconia and powder doped with 3 and 5 mol % Al_2O_3) or cubic (for powder doped with 15 mol % Al_2O_3). The changes of the lattice parameters and c/a ratio, presented in Figure 3, show that tetragonality decreases with increasing doping level and closely approaches $c/a = 1$ already for the as-synthesized powder doped with 5 mol % Al_2O_3. The microstrain in the CVS doped nanopowders increases simultaneously with decreasing tetragonality (Table 1). The microstrain is 0.0041, 0.0093, and 0.0163 in the pure zirconia and powder doped with 3 and 5 mol % Al_2O_3, respectively. A small relaxation of the microstrain is observed with the formation of cubic ZrO_2 in the CVS nanopowder doped with 15 mol % Al_2O_3 (Table 1). The fraction of the monoclinic ZrO_2 decreases with increasing alumina content; that is, it is 22 vol % in the pure ZrO_2, 16 vol % in the sample with 5 mol % Al_2O_3, and 0 vol % in the 15 mol % Al_2O_3 sample (Table 1). The average crystallite size obtained by the Rietveld refinement ranges from 4 to 5 nm (Table 1).

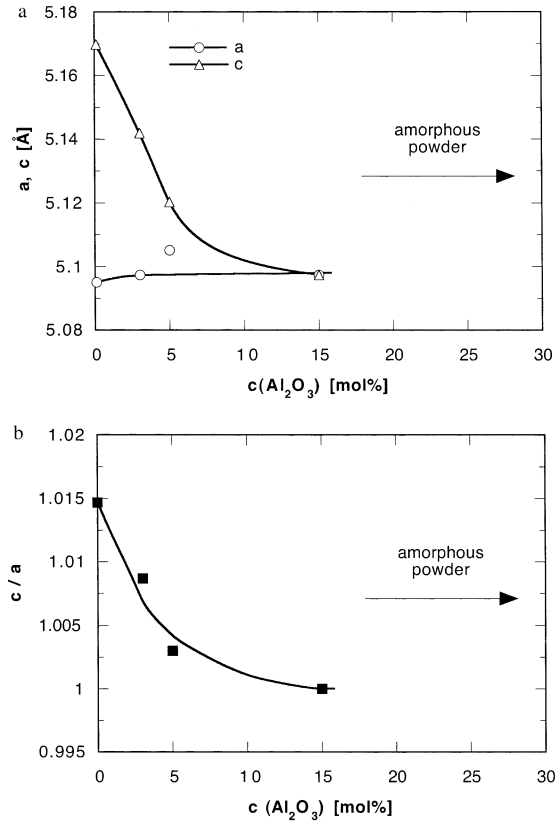

Figure 3. (a) Lattice parameters and (b) c/a ratio as a function of alumina content in the as-synthesized CVS doped zirconia nanopowders.

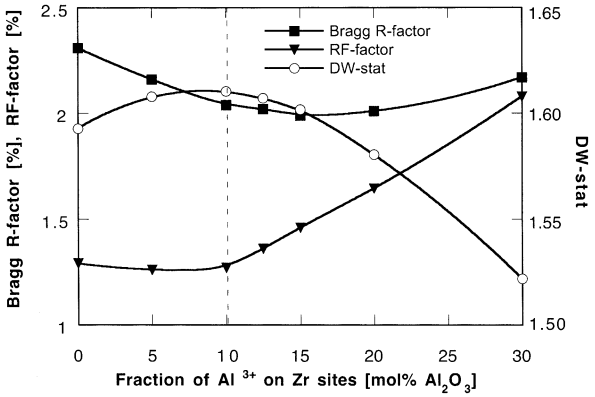

Figure 4. Rietveld refinement parameters (Bragg R-factors, RF-factors, and DW-stat) versus quantity of Al^{3+} ions on Zr sites in the tetragonal zirconia lattice (calculated in mol % Al_2O_3), for the CVS zirconia doped with 30 mol % Al_2O_3 and annealed at 1000 °C.

Characteristics of Annealed Powders. The Rietveld analysis of diffractograms of the annealed powders was performed with the pure monoclinic zirconia, the tetragonal or cubic ZrO_2 structure with different fractions of Al atoms on Zr sites, and the corresponding quantity of the amorphous and/or transitional η-, γ-, or θ-alumina phase (formed by the rest of the Al^{3+} ions). Again, refinements with the minimum Bragg R-factor and RF-factor and the maximum DW-stat factor were selected as best fits. An example is represented in Figure 4 for the CVS zirconia sample doped with 30 mol % Al_2O_3 annealed at 1000 °C. The data points in Figure 4 correspond to the Rietveld refinements obtained for different fractions of Al atoms on Zr sites (presented as

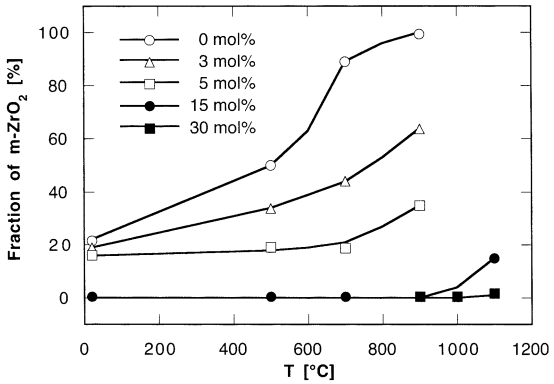

Figure 5. Volume fraction of the monoclinic ZrO_2 versus annealing temperature for the CVS doped zirconia.

x-axis and calculated as Al_2O_3 content in mol %). For Al fractions less than the doping level (for $x < 30$ mol % Al_2O_3) the transitional alumina phase was also included in the analysis. The best fit for the zirconia doped with 30 mol % Al_2O_3 and annealed at 1000 °C is obtained when only one-third of the Al^{3+} ions are on Zr sites (dashed line in Figure 4) and the rest of the Al^{3+} ions form a separate alumina phase. Generally, the Rietveld analysis clearly shows that cubic ZrO_2 is never observed as a best model in the refinements of the annealed CVS powders and that the fraction of Al atoms in the tetragonal ZrO_2 is usually smaller than the doping level. It should be mentioned that it was difficult to distinguish between the transitional γ- and η-Al_2O_3 phases as the corresponding XRD peaks are very weak and the lattice parameters of the two spinel-type structures are very close.[15,16]

The annealing experiments of the CVS pure ZrO_2 powder[12] showed that the transformation from tetragonal to monoclinic symmetry is almost complete at 800 °C (Figure 5). However, the results presented in Figures 5 and 6 show that even a small quantity of Al_2O_3 (up to 5 mol %) considerably increases the stability of the tetragonal ZrO_2. Thus, fractions of the monoclinic phase in the 3 and 5 mol % Al_2O_3 doped powders annealed at 700 °C are 44 and 19 vol %, respectively. Complete stabilization of the tetragonal ZrO_2 in the annealed nanopowders is achieved at higher alumina contents (≥15 mol % Al_2O_3). During annealing, the cubic zirconia solid solution observed in the as-synthesized zirconia doped with 15 mol % Al_2O_3 first transforms at 500 °C into the metastable tetragonal solid solution, but the transformation to the monoclinic symmetry starts only at temperatures higher than 900 °C (Figure 5). The highly doped, amorphous, zirconia nanopowders crystallize at about 800 °C into a single-phase solid solution with *t*-ZrO_2 structure (zirconia doped with 30 mol % Al_2O_3) or at about 850 °C into a two-phase system consisting of *t*-ZrO_2 and η-/γ-Al_2O_3 (zirconia doped with 50 mol % Al_2O_3). The transformation to the monoclinic symmetry in both powders starts only at 1100 °C (Figures 5 and 6). These results are consistent with data already published for the wet-chemically synthesized materials with the same alumina content.[4,8]

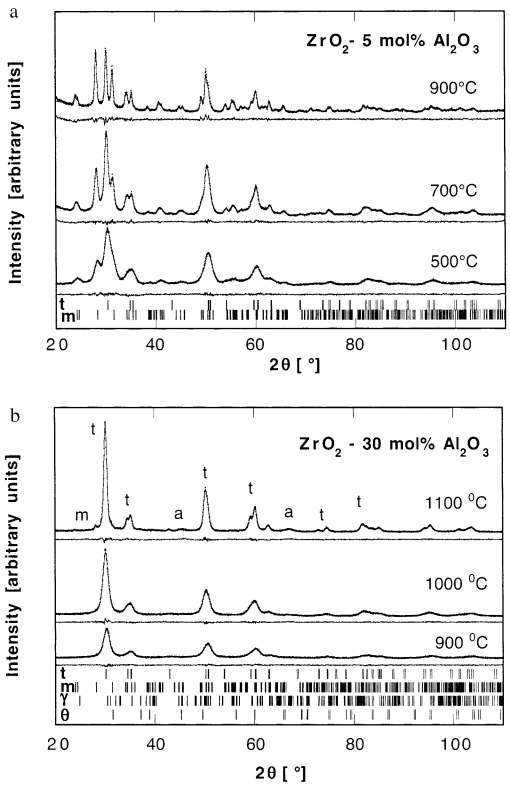

Figure 6. XRD powder patterns of the CVS zirconia doped with (a) 5 and (b) 30 mol % Al_2O_3 annealed at different temperatures, indicated in plots (letters "t", "m", and "a" indicate tetragonal ZrO_2, monoclinic ZrO_2, and transitional Al_2O_3 phases, respectively). Lines through data points are the best Rietveld, refinements, lines below the data are the corresponding residual signals, vertical lines are Bragg positions for the different phases.

At higher annealing temperatures segregation of alumina phases was observed by XRD (Figure 6) and confirmed by Rietveld analysis for highly doped powders. X-ray diffraction patterns of nanopowders annealed at 1000 °C (15 and 30 mol % Al_2O_3 samples) and even 850 °C (50 mol % Al_2O_3 sample) exhibit weak peaks at about 45° and 66° 2θ, corresponding to transitional alumina phases. However, Rietveld analysis shows that segregation, that is, the decrease of occupation of Al^{3+} on Zr sites in the tetragonal lattice, starts already at 700 and 900 °C for nanopowders doped with 15 and 30 mol % Al_2O_3, respectively. A similar discrepancy was observed in the wet-chemical synthesized zirconia/alumina nanopowders,[8] where the onset of phase partitioning was detected by electron diffraction before (at lower temperature) transitional γ-Al_2O_3 was detected by XRD. Since segregation starts at the local level, initially no crystalline structures large enough to be detected by XRD are formed. The Rietveld analysis shows that the best fit for highly doped nanopowders annealed at 900 and 1000 °C was obtained with the transitional η- or γ-Al_2O_3 while at 1100 °C the θ-Al_2O_3 phase was detected.

The fraction of Al^{3+} on Zr sites in the tetragonal zirconia lattice of the doped CVS nanopowders as a function of temperature and doping level is presented in Figure 7. The fraction is equal to the doping level only for the nanopowder with low alumina content and for the 15 mol % Al_2O_3 sample annealed at temperatures

(15) Zhou, R.-S.; Snyder, R. L. *Acta Crystallogr.* **1991**, *B47*, 617.
(16) Winterer, M. *Nanocrystalline Ceramics—Synthesis and Structure*; Springer: Heidelberg, 2002.

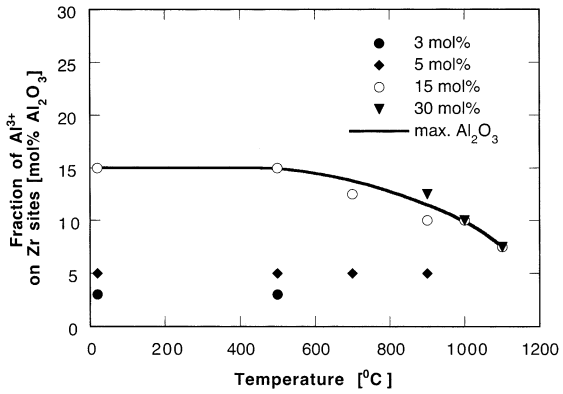

Figure 7. Fraction of Al^{3+} on Zr sites (calculated on mol % Al_2O_3) in the tetragonal/cubic zirconia lattice at different temperatures, obtained by the best Rietveld refinement.

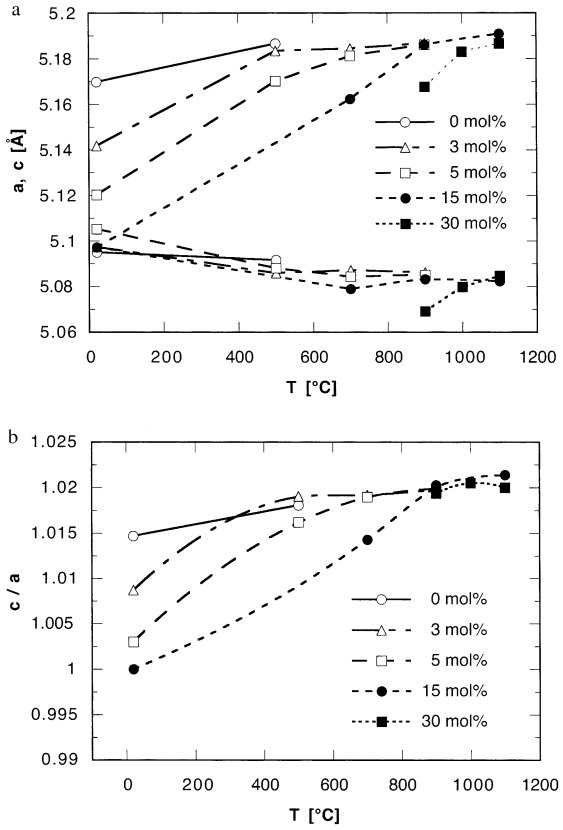

Figure 8. (a) Lattice parameters and (b) *c*/*a* ratio as a function of annealing temperature for zirconia with different alumina content.

below 700 °C. In the highly doped powders at higher annealing temperatures only a fraction of Al^{3+} ions is remaining on the Zr sites independent of the alumina doping level (solid line in Figure 7). In conclusion, the Rietveld analysis of the annealed nanopowders shows that the maximum solubility is about 15 mol % Al_2O_3 (i.e., 26 at. % Al).

Changes in the lattice parameters and *c*/*a* ratio during annealing of the CVS doped powders are presented in Figure 8. The changes are very pronounced at low annealing temperatures and even at 500 °C tetragonality increases considerably and the *c*/*a* ratio becomes higher than 1.010. Figure 8b illustrates that an increased alumina content shifts the *c*/*a* ratio toward lower values. The tetragonality of CVS powders doped

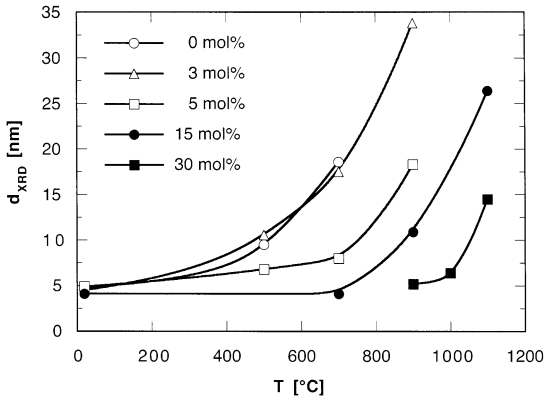

Figure 9. Crystallite size versus annealing temperature for the CVS doped zirconia.

Table 2. Average Unit-Cell Volume (V_{cell} (Å^3)) of the CVS Doped Zirconia Nanopowders as a Function of Annealing Temperature

	nominal Al_2O_3 content (mol %)					
T (°C)	0	3	5	15	30	50
20	134.21 (30)	133.60 (35)	133.45 (44)	132.44 (14)		
500	134.38 (7)	134.08 (5)	133.85 (9)			
700		134.17 (3)	133.95 (3)	132.95 (6)		
900		134.19 (2)	134.10 (3)	134.00 (4)	132.79 (8)	
1000					133.70 (5)	133.09 (6)
1100				134.08 (2)	134.10 (2)	

with identical alumina content increases with annealing temperature and approaches $c/a = 1.021$, that is, $a = 5.085$ Å and $c = 5.190$ Å. Average unit-cell volumes, calculated from the lattice parameters, are presented in Table 2 for the as-synthesized and annealed powders. The unit-cell volume decreases with increasing alumina content in the as-synthesized powder and displays the same trend during annealing. This is in contrast to an observed linear increase of the unit-cell volume (consistent with a linear increase of the cubic lattice parameter *a* from 5.095 to 5.129 Å) with increasing alumina content in cubic zirconia−alumina solid solutions.[4] However, as the solid solution is formed by substitution of larger Zr^{4+} ions with smaller Al^{3+} ions, it seems reasonable to expect a decrease of the unit-cell volume with increasing alumina content, supporting the data in Table 2.

The widths of the XRD reflections for CVS zirconia powders change with annealing temperature and doping level. The Rietveld analysis was used to distinguish and determine the corresponding size and microstrain contributions to the line broadening. Changes in the tetragonal ZrO_2 crystallite size with annealing temperature are presented in Figure 9. The average crystallite size increases with annealing temperature and decreases considerably with increasing alumina content. Thus, highly doped ZrO_2 powders have very small crystallite sizes (<10 nm), even at annealing temperatures as high as 1000 °C (Figure 9). Changes in the microstrain in tetragonal ZrO_2 crystallites, estimated by Rietveld analysis, are shown in Figure 10. As is expected, at the same annealing temperature, the microstrain is higher in highly doped powder. Strain relaxation is observed with increasing annealing temperature, in agreement with the decrease of the occupation of Al^{3+} on Zr sites in the tetragonal lattice.

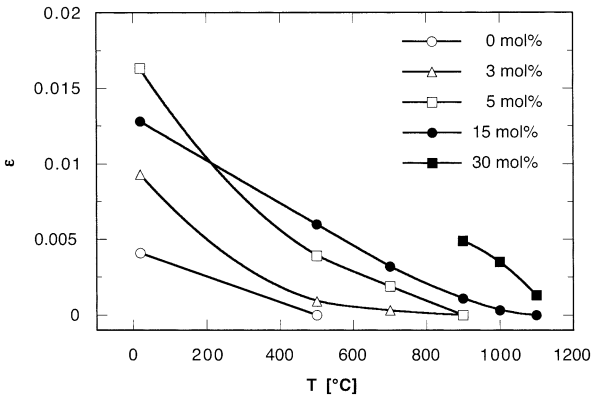

Figure 10. Microstrain versus annealing temperature for the CVS doped zirconia.

Discussion

According to the presented results, it is clear that doping of zirconia with Al^{3+} ions stabilizes tetragonal or cubic zirconia polymorphs. This can be explained by the formation of ZrO_2/Al_2O_3 solid solutions already mentioned in the literature.[4,8,17] Analogous to Y^{3+}, and other trivalent cations forming solid solutions with zirconia, Al^{3+} ions substitute Zr^{4+} ions. The local charge balance can be maintained by creating one oxygen vacancy (V_O^{2-}) for every two Al^{3+} ion introduced.

Depending on the alumina content, the as-synthesized CVS zirconia doped nanopowders are crystalline (≤15 mol % Al_2O_3) or amorphous (for 30 and 50 mol % Al_2O_3). On average already at 5 mol % Al_2O_3 each Zr^{4+} ion has one aluminum neighbor in the next cation shell and at 30 mol % every second Zr^{4+} ion is substituted by Al^{3+}. Therefore, the crystalline zirconia structure can no longer accommodate the aluminum ions and it is reasonable to distinguish between two structural models for the ZrO_2/Al_2O_3 solid solutions.[17] At low alumina contents Al^{3+} ions randomly substitute some of the Zr^{4+} ions and oxygen vacancies are created to maintain the local charge balance. Thus, a crystalline structure in the as-synthesized nanopowders can be formed. In contrast, at high alumina contents a more disordered, amorphous structure of the as-synthesized nanopowders is produced, consisting of small-scale Al−O−Al units larger than those predicted statistically in the solid solution. The border between amorphous and crystalline structures depends on the synthesis conditions and can probably be moved toward higher alumina content by optimizing the CVS parameters.

There is an apparent discrepancy in the literature concerning the type of dominant zirconia phase (i.e., solid solution) and the Al_2O_3 solubility level in ZrO_2/Al_2O_3 systems. It was shown that as-synthesized solid solutions prepared by laser evaporation of ZrO_2 and Al_2O_3 microspheres have tetragonal symmetry,[10] whereas wet-chemically synthesized amorphous ZrO_2/Al_2O_3 crystallizes as a single-phase cubic[4] or a tetragonal[8] zirconia solid solution. This discrepancy could be related to the different processing techniques employed. However, due to the enormous XRD line broadening in nanocrystalline powders, it is difficult to differentiate between cubic and tetragonal. Therefore, Rietveld refinements of data with sufficient statistics are essential for obtaining detailed and accurate structural information for doped nanocrystalline zirconia powders. The presence of the tetragonal zirconia solid solution in samples doped with 3 and 5 mol % Al_2O_3 and the single-phase cubic zirconia solid solution in the powder doped with 15 mol % Al_2O_3 additionally confirms that Al^{3+} behaves similarly to Y^{3+}, which forms the tetragonal zirconia solid solution at a low doping level (about 3 mol % Y_2O_3) and the cubic solid solution at a higher doping level (>6 mol % Y_2O_3).[18,19] A maximum solubility of about 15 mol % Al_2O_3 (i.e., 26 at. % Al) is observed in the CVS doped nanopowders, which is considerably lower than 40 mol % (i.e., 57 at. % Al) reported by Balmer et al.[8] In addition to the reasons mentioned above, this discrepancy may exist because of Balmer's two very strict assumptions: first, that during crystallization of highly doped amorphous powders (with 20 and 40 mol % Al_2O_3) all Al atoms are located on Zr sites in the tetragonal ZrO_2 lattice and, second, that the transitional alumina phase was formed only with outgoing Al^{3+} ions from the host ZrO_2 lattice in the second exothermic process detected by differential thermal analysis.[8]

Even though there are some similarities between Al^{3+} and Y^{3+} ions as dopants in zirconia, it should be pointed out that the tetragonal or cubic zirconia solid solutions in the Al_2O_3/ZrO_2 system are *metastable* at all temperatures. In contrast, the solid solutions in the Y_2O_3/ZrO_2 system are *thermodynamically stable* at high temperatures and metastable at low temperatures. Additionally, contrary to the Y^{3+} ion (r_{ion} = 0.93 Å), which is larger than Zr^{4+} (r_{ion} = 0.8 Å), resulting in solid solutions with larger unit-cell volume than pure ZrO_2,[1] the unit cell volume decreases in Al-doped zirconia because the Al^{3+} is smaller (r_{ion} = 0.5 Å) than Zr^{4+} (Table 2).

The results presented here indicate that the CVS zirconia doped nanopowders have promising characteristics for good sinterability at reduced grain growth. They are able to produce metastable solid solutions which can segregate at high temperatures on an ultrafine scale limiting the grain growth of zirconia. Thus, vacuum sintering of the CVS zirconia doped with 3 and 5 mol % Al_2O_3 at 1000 °C for 1 h results in fully dense, transparent ceramics with grain sizes of about 40−45 nm.[13] Higher alumina contents (>5 mol % Al_2O_3) further suppress the zirconia grain growth, but also retards the densification process.[13]

Conclusions

Rietveld analysis of XRD data enabled the detailed investigation of the structure of as-synthesized and annealed CVS zirconia nanopowders doped with up to 50 mol % Al_2O_3. Doping with Al^{3+} ions decreases the fraction of monoclinic ZrO_2 and stabilizes tetragonal or cubic ZrO_2 through formation of ZrO_2/Al_2O_3 solid solutions. Solid solutions are formed by incorporation of Al^{3+} ions in the fluorite-type zirconia structure by substituting Zr^{4+} ions and creating oxygen vacancies to maintain local charge balance. The tetragonal zirconia solid

(17) Balmer, M. L.; Eckert, H.; Das, N.; Lange, F. F. *J. Am. Ceram. Soc.* **1996**, *79*, 321.

(18) Scott, H. G. *J. Mater. Sci.* **1975**, 10, 1527.

(19) Stubican V. S. *Science and Technology of Zirconia III, Advances in Ceramics, Vol 24*; Somiya S., Yamamoto N., Hanagida H., Eds.; The American Ceramics Society: Westerville, OH, 1988; p 71.

solution is obtained in the as-synthesized nanopowders doped with 3 and 5 mol % Al_2O_3, the cubic zirconia solid solution is formed in the nanopowder with 15 mol % Al_2O_3, and the nanopowders with higher alumina content (30 and 50 mol % Al_2O_3) are amorphous. The formation of metastable solid solutions is possible by CVS because it is a highly nonequilibrium process.[16] During annealing Al^{3+} ions diffuse out of the zirconia lattice, causing an increase of the ZrO_2 tetragonality, formation of monoclinic zirconia, and transitional alumina phases by segregation. The observed maximum solubility of alumina in the cubic/tetragonal zirconia is about 15 mol % Al_2O_3 (or 26 at. % Al). Al^{3+} ions behave similarly to Y^{3+} ions as dopants in zirconia, with the important difference that the tetragonal or cubic zirconia solid solutions in the ZrO_2/Al_2O_3 system are metastable at all temperatures, whereas the solid solutions in the ZrO_2/Y_2O_3 system are stable at high and metastable at low temperatures.

Acknowledgment. The authors would like to thank the Alexander von Humboldt Foundation for the research fellowship for Vladimir V. Srdić and the German Science Foundation for financial support.

CM021303Q